Single-Molecule Elasticity Measurements of the Onset of Excluded Volume in Poly(Ethylene Glycol)

Andrew Dittmore,[1] Dustin B. McIntosh,[2] Sam Halliday,[3] and Omar A. Saleh[1,*]

[1]*Materials Department, University of California, Santa Barbara, California 93106, USA*
[2]*Physics Department, University of California, Santa Barbara, California 93106, USA*
[3]*Materials Department, University of Oxford, United Kingdom*

(Received 29 April 2011; published 27 September 2011)

A polymer must reach a certain size to exhibit significant excluded-volume interactions and adopt a swollen random-walk configuration. We show that single-molecule measurements can sense the onset of swelling by modulating the effective chain size with force: as the force is reduced from a large value, the polymer is first highly aligned, then a Gaussian coil, then finally a swollen chain, with each regime exhibiting a distinct elasticity. We use this approach to quantify the structural parameters of poly(ethylene glycol) and show that they vary in the expected manner with changes in solvent.

DOI: 10.1103/PhysRevLett.107.148301 PACS numbers: 36.20.Ey, 61.25.hp, 82.37.Rs, 87.15.La

The random-walk configuration of a polymer in good solvent becomes self-avoiding when the total energy of the repulsive pairwise monomer interactions exceeds the thermal energy, k_BT. When quantified within Flory theory, this criterion predicts that self-avoidance is only significant when the polymer's extent (i.e., radius of gyration), R, exceeds a length scale termed the thermal blob size [1], b, given by $b \sim l^4/v$, where l is the polymer's Kuhn length and v is the excluded-volume parameter that accounts for the strength of monomer interactions. For $R < b$, self-avoidance is not significant and the polymer assumes an ideal random-walk configuration, $R \sim N^{1/2}$, where N is the number of statistical monomers. Inversely, for $R > b$, self-avoidance is significant and the polymer assumes swollen, real configurations that are well-approximated by Flory's scaling law, $R \sim N^{3/5}$ [2]. Thus, certain polymers (depending on the values of l and v, and so on polymer structure and solvent quality) will display an ideal-to-real transition with increasing chain length.

Quantifying the crossover from ideal-to-real behavior is of fundamental importance to describing the structure of the chain. This determination affects a multitude of applications, especially as many biologically and technologically important polymers are relatively short, including RNAs, proteins, and soluble synthetic polymers. However, measuring the ideal-to-real transition has proven challenging using standard dilute-solution polymer characterization methods [3], such as light scattering, osmotic pressure, or rheology. Such methods require testing of many monodisperse polymer samples over a wide range of molecular weights, even though the properties of polymer solutions derive from the fundamental length scales within a single chain.

Here, we demonstrate that the elastic response of a single polymer under small tension can provide estimates of its Kuhn length, thermal blob size, and excluded-volume parameter. Conceptually, this capability arises from two considerations. (i) A constrained polymer is well-described by the ''blob'' picture of Pincus and de Gennes [4,5]: application of a force f effectively breaks up the chain into a series of independent fragments, each of extent given by the tensile screening length, $\xi \sim k_BT/f$. Thus, varying the force varies the fragment size, allowing measurement of the characteristics of a range of chain lengths without the need to synthesize a variety of chains. (ii) The low-force elastic response of real and ideal chains differs significantly, permitting precise identification of each regime. In particular, the force-extension behavior of a self-avoiding chain follows $L \sim f^{2/3}$ as predicted by Pincus [4] and confirmed experimentally [6,7]; this is distinct from the $L \sim f$ entropic-spring behavior of an ideal chain.

This conceptual framework predicts transitions in elastic response when ξ is equal to a characteristic length scale of the polymer; thus, by measuring elastic transitions, we can quantify the polymer's microscopic structure. We expect three elastic regimes (Fig. 1) [7,8]: At high forces, the chain is highly aligned to the force and the extension asymptotically approaches the contour length. As the force is decreased, a first transition occurs at $\xi^* = l$, below which the polymer is a chain of small random-walk blobs with ideal, $L \sim f$, elastic response. At still lower forces, the blob size grows and a second transition occurs at $\xi^{**} = b$. At this point, in good solvent the polymer becomes swollen with $L \sim f^{2/3}$ elastic response, while in poor solvent it undergoes a discontinuous transition to a collapsed globule [9]. The values of l and b, estimated from the measured ξ^* and ξ^{**}, can in turn be used to estimate the excluded-volume parameter from $|v| \sim l^4/b$.

To validate this framework, we measured the elasticity of single molecules of poly(ethylene glycol) (PEG) using magnetic tweezers. Elasticity measurements were performed using a custom-built apparatus based on an inverted microscope and capable of applying constant forces to magnetic colloids while tracking their 3D position (and

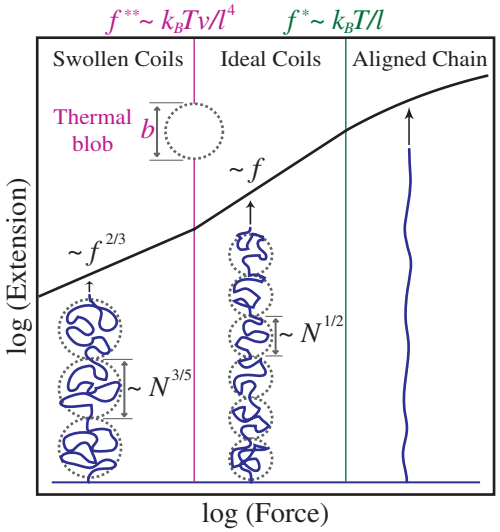

FIG. 1 (color). Single-molecule elasticity method for sensing the onset of excluded volume with polymer size, which varies inversely with force. The microscopic parameters l, v and b can be obtained from the measured transition forces.

thus polymer extension) with nanometer precision in real time [10]. Force calibration was determined in advance using 1 μm Dynal beads tethered to long DNA molecules [11]. We found a minimal variation across the bead population in the applied force (less than 10% for forces of 0.2–20 pN) which is due to small size differences between beads. Importantly, this mechanism of variation means that our analysis of power-law elastic behavior is robust against systematic errors in force calibration: the force applied to any given bead will differ from the mean by a small constant factor across all forces, resulting in a lateral shift of the extension vs force curve on log-log axes, but no change in the exponent of a power law.

Biotin-PEG-maleimide, MW = 80000, PD = 1.1 (GPC), was purchased from JenKem Technology as a powder, and vacuum sealed to protect the labile functional groups from hydrolysis in air. We dissolved 100 mg of powder in 10 ml anhydrous dimethylformamide in an opaque bottle sealed with argon to completely eliminate moisture and stored this stock solution at 4 °C. PEG chains were immobilized to the surface of a glass flow cell by maleimide/thiol chemistry at a grafting density of $\sim$1 per 100 μm^2: After treating the glass with (3-mercaptopropyl)-trimethoxysilane, a small volume of stock PEG was drawn with a needle and diluted to $\sim$20 pM in 10 mM phosphate buffer, pH 7. This solution was incubated with the glass for 15 min; the resulting end-grafted chains were then tethered to streptavidin-coated paramagnetic beads through the biotin moiety at the free end. Good-solvent testing was performed in 10 mM phosphate buffer, pH 7 with 0.1% Tween-20 surfactant included to prevent the beads from sticking to the surface.

Using low forces gives short polymer extensions, requiring us to carefully control for possible systematic errors in the extension measurement. First, the beads were introduced to the flow cell in a uniform magnetic field, then tested by rotating the field, to remove errors associated with the bead's curvature [12]; this test also served to identify and discard beads tethered by multiple polymers through their anomalous extension change upon rotation [13]. Next, we recognized that the presence of asperities on the rough bead surface can contribute a constant positive or negative error to the length of a given tether. Reasoning that this random source of error should be centered at zero for a population of tethers, we report the *mean* $\pm$ *standard deviation* of the analyzed parameters for five exemplary PEG molecules in good solvent.

In accordance with the scaling predictions described above [7,8] (Fig. 1), our measurements of PEG elasticity in good solvent display multiple distinct elastic regimes [Fig. 2(a)]. Starting from high forces, we observe the following:

Highly aligned regime.—Between $\sim$5 and $\sim$20 pN, the PEG elasticity is well-fit by the Marko-Siggia wormlike chain (WLC) model [14]. The range of best-fit contour lengths, $L_0 = 570 \pm 56$ nm, is consistent with that expected for an 80 kDa PEG chain in water [15,16]. The best-fit persistence length, $p = 0.47 \pm 0.02$ nm, is slightly larger than previously reported from high-force (> 25 pN) AFM testing [17]. This is consistent with recent theories that indicate stretching a polymer at high forces leads to deformations that return systematic underestimates of p [18–20].

Indeed, it is likely that even moderate forces deform the polymer, as we observe a deviation of the elastic response from WLC behavior. Beginning near $f = k_B T/(2p) \approx 4.4$ pN, the deviation consists of an extension larger than that predicted from the WLC fit, which we attribute to a local change in chain structure and flexibility. We characterize this deviation by comparing the persistence length p (the characteristic length over which tangents to the polymer become uncorrelated), obtained at high forces, to the Kuhn length l (the step size of the statistically equivalent random-walk coil), obtained at intermediate forces. Within a WLC model we expect to measure $l = 2p$; however, the deviation causes $l > 2p$ at forces below 2 pN, consistent with a more rigid polymer in the ideal-coil regime.

Ideal-coil regime.—Between $\sim$0.7 and $\sim$2 pN, the elastic response is linear: the best-fit power law returns $L \sim f^{0.99 \pm 0.03}$. A linear response indicates that PEG forms into a series of ideal coils. Using the entropic-spring model and setting L_0 to the value found from the WLC fits, we can relate the measured slope, $\frac{d}{df}(L/L_0)$, to the Kuhn length through $l = 3k_B T \frac{d}{df}(L/L_0)$. This gives $l = 1.1 \pm 0.1$ nm, precisely the value measured by dilute-solution light scattering and by neutron scattering in PEG melts [2,21], and consistent with the transition force $k_B T/l \sim f^*$.

Swollen-coil regime.—As the tension is lowered below $\sim$0.7 pN, excluded-volume interactions overcome the

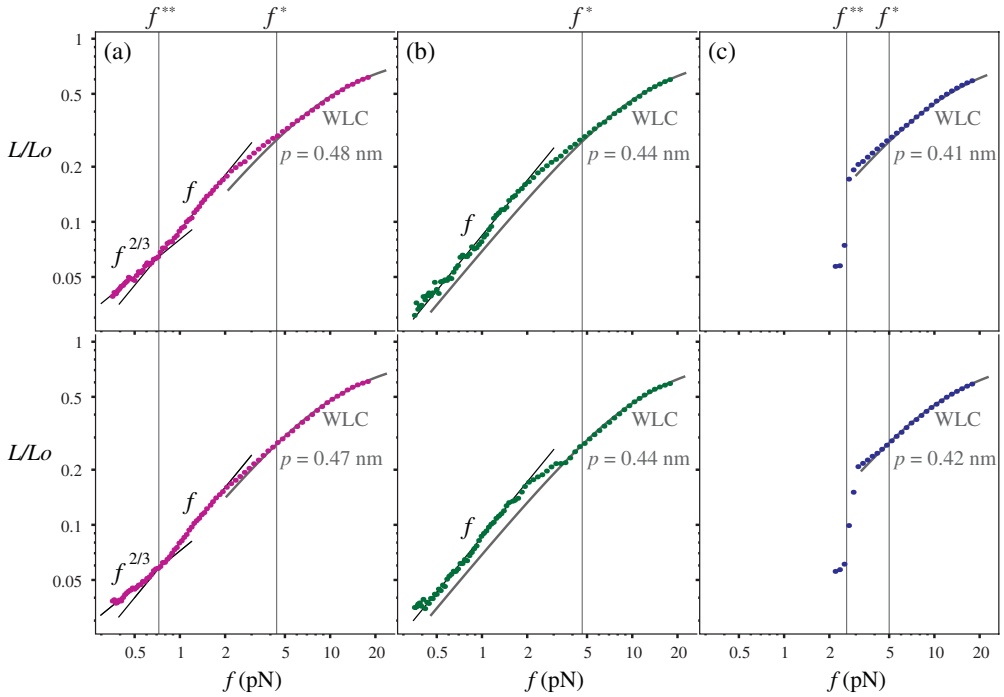

FIG. 2 (color). Data of normalized length versus tensile force for representative single PEG chains in (a) good solvent, (b) theta solvent, and (c) poor solvent. The solid lines indicate the predicted power-law behavior in the low-force regimes and fits to the wormlike chain model at high force. The solvent-dependent transition forces are also indicated. Under theta-solvent conditions, the Pincus regime disappears as $\upsilon \to 0$. In good and poor solvent, the measured f^{**} values give $\upsilon \approx 0.2$ nm^3 and $\upsilon \approx -0.5$ nm^3, respectively.

thermal energy and the coils swell. At the onset of excluded volume the elasticity changes appreciably, with a best-fit power-law, $L \sim f^{0.69\pm0.08}$, that is in excellent agreement with the $L \sim f^{2/3}$ Pincus prediction. We obtain the thermal blob size $b \approx 6$ nm from the crossover force $f^{**} = 0.74 \pm 0.05$ pN and the scaling relation $b \sim k_B T/f^{**}$. In turn, from $\upsilon \sim l^4/b$, we estimate the excluded-volume parameter to be $\upsilon \approx 0.2$ nm^3.

We are thus able to determine L_0, p, l, b, and υ from a direct measurement on a single polymer in good solvent. To corroborate these results, we repeated the elastic measurements in solvents of lower quality. In particular, since PEG is known to intimately associate with the hydrogen-bonded network of water [15,22–24], we chose to test PEG in potassium salts [25]: potassium is ranked as highly precipitating in the Hofmeister series and known to strongly disrupt water structure.

In 1 M KCl, the elastic measurements no longer show a swollen-coil regime; we measure linear-elastic behavior throughout the low-force range [Fig. 2(b)], indicative of a theta point of the system. This is consistent with the expectation: the perturbed water structure decreases the repulsion between PEG monomers, lowering the excluded-volume parameter to zero. To more aggressively decrease the solvent quality, we repeated the measurements in 0.4 M K_3PO_4 salt (we note that, in these conditions, the solution became highly alkaline). We found that PEG undergoes poor-solvent collapse [Fig. 2(c)]: as the constant force is lowered, attractive contacts form and condense the polymer, indicative of a negative excluded-volume parameter. The chain begins to jump stochastically between an aligned state and a collapsed-globule state through a narrow range of intermediate constant forces, then remains in the collapsed state at lower forces. As predicted [9], this behavior points to a collapse mechanism dominated by the surface tension of the polymer-solvent interface. For the two curves shown in Fig. 2(c), the collapse occurs at $f^{**} \approx 2.5$ pN, from which we estimate $\upsilon \approx -0.5$ nm^3.

Our results support a general phase diagram for the configuration of a polymer (Fig. 3), in which the effective chain size is modulated by applied tension and the quality of solvent is parameterized by υ. The highly aligned–ideal-coil transition occurs at constant force, $f^* l/k_B T \sim 1$. The ideal-coil–real-coil and ideal-coil–collapsed-globule transitions occur at a force linearly dependent on υ, $f^{**} l/k_B T \sim |\upsilon|/l^3$. For PEG in particular, a portion of the ideal-coil regime is obscured by the structural transition near $f \approx 4$ pN.

We have shown that gentle stretching is uniquely sensitive to details of real polymer structure. Previous measurements of PEG elasticity showed that the polymer has solvent-mediated superstructure and that the asymptotic approach to its contour length is well described by the Marko-Siggia wormlike chain model [16,17]. Although

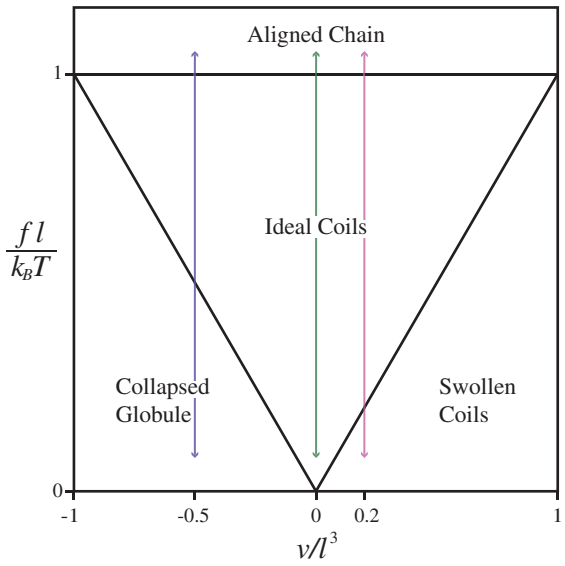

FIG. 3 (color). Phase diagram of polymer configuration for a range of tensile forces and solvent qualities. Boundaries follow the $f^* l/k_B T \sim 1$ and $f^{**} l/k_B T \sim |v|/l^3$ scaling predictions; the f^{**} transition is continuous for $v > 0$ and discontinuous for $v < 0$. The vertical lines indicate the conditions determined for the data in Fig. 2.

these results exemplify the power of single-molecule force spectroscopy in probing local structural details, sensing b and v requires access to longer length scales, meaning lower forces. Moreover, the low-force stability of magnetic tweezers allows us to observe phenomena such as chain collapse, and avoids the systematic underestimates of l caused by forcing the chain into highly strained conformations.

The confining bead and glass surfaces apparently have little to no effect on the measured elasticity. This is not surprising when the forces are high and there are many internal tension blobs that act independently. However, even as the blob size slowly becomes a larger fraction of the chain, the low-force elastic response persists as $L \sim f^{2/3}$ (swollen) in good solvent, or as $L \sim f$ (ideal) in theta solvent, to the lowest forces measured.

Using low-force stretching, we observed the ideal-to-real transition in PEG elastic behavior. In comparison, single-stranded DNA (ssDNA) shows no intermediate ideal-coil regime [6,7]; instead the elasticity of ssDNA transitions directly from the highly-aligned to the swollen regime. We attribute the difference to the geometry of the statistical segments: for spherical segments, $v \sim l^3$, the thermal blob size is identical to the Kuhn length, $b \sim (l^4/v) \sim l$, and no ideal-coil elastic regime is expected (Fig. 3). The Kuhn segments of ssDNA are largely defined by isotropic electrostatic interactions [6,7] and are thus approximately spherical. In contrast, our measurements of v and l of PEG indicate the statistical monomers are rodlike with an aspect ratio of roughly 5, in agreement with prior estimates [2]. Thus, for PEG, $v < l^3$ and $b > l$, leading to an intervening ideal elastic regime. The key role of aspect ratio is further confirmed by studies of denatured polypeptides [26], which are swollen at any length of peptide chain. The lack of ideal coils in proteins can be explained by the large amino-acid side chains, which produce an effective chain diameter and approximately spherical statistical segments. Similarly, the Kuhn length of bottle-brush polymers is directly proportional to the chain diameter, leading to an aspect ratio near unity and the lack of an ideal-coil regime [27]. In the opposite limit, double-stranded DNA (dsDNA) has an extraordinarily large aspect ratio (~ 50); correspondingly, elastic measurements of dsDNA have not indicated any effects of swelling, which presumably only occur for a range of contour lengths and forces that have not been explored [14].

In summary, we have demonstrated that single-molecule measurements are capable of probing real polymer structure on various length scales. By scanning force, we have confirmed that multiple elastic regime transitions are in agreement with scaling predictions and signify solvent-dependent structural parameters. Our low-force technique is sensitive to long-range interactions; we have directly observed the onset of excluded volume in PEG, finding that PEG in good solvent is swollen only if longer than roughly 100 ethylene oxide units, or 30 Kuhn lengths.

We thank Phil Pincus and Alexander Grosberg for enriching discussions, and Frank Leibfarth for help in preparing the polymer solution for long-term storage. This work was supported by the National Science Foundation under Grant DMR-1006737, the MRSEC program under Grant DMR05-20415, and by support from UCSB Materials Research Laboratory CSP Technologies to A. D.

*saleh@engineering.ucsb.edu

[1] D. W. Schaefer, J. F. Joanny, and P. Pincus, Macromolecules **13**, 1280 (1980).
[2] M. Rubinstein and R. H. Colby, *Polymer Physics* (Oxford University Press, USA, 2003).
[3] H. Fujita, Macromolecules **21**, 179 (1988).
[4] P. Pincus, Macromolecules **9**, 386 (1976).
[5] P. G. de Gennes, *Scaling Concepts in Polymer Physics* (Cornell University, Ithaca, 1979).
[6] O. A. Saleh *et al.*, Phys. Rev. Lett. **102**, 068301 (2009).
[7] D. B. McIntosh, N. Ribeck, and O. A. Saleh, Phys. Rev. E **80**, 041803 (2009).
[8] R. R. Netz, Macromolecules **34**, 7522 (2001).
[9] A. Halperin and E. B. Zhulina, Europhys. Lett. **15**, 417 (1991).
[10] N. Ribeck and O. A. Saleh, Rev. Sci. Instrum. **79**, 094301 (2008).
[11] C. Gosse and V. Croquette, Biophys. J. **82**, 3314 (2002).
[12] D. Klaue and R. Seidel, Phys. Rev. Lett. **102**, 028302 (2009).
[13] T. R. Strick *et al.*, Biophys. J. **74**, 2016 (1998).
[14] J. F. Marko and E. D. Siggia, Macromolecules **28**, 8759 (1995).

[15] J. E. Mark and P. J. Flory, J. Am. Chem. Soc. **87**, 1415 (1965).
[16] F. Oesterhelt, M. Rief, and H. E. Gaub, New J. Phys. **1**, 6 (1999).
[17] F. Kienberger *et al.*, Single Mol. **1**, 123 (2000).
[18] L. Livadaru, R. R. Netz, and H. J. Kreuzer, Macromolecules **36**, 3732 (2003).
[19] N. M. Toan and D. Thirumalai, Macromolecules **43**, 4394 (2010).
[20] A. V. Dobrynin, J. M. Y. Carrillo, and M. Rubinstein, Macromolecules **43**, 9181 (2010).
[21] G. D. Smith *et al.*, Macromolecules **29**, 3462 (1996).
[22] R. Kjellander and E. Florin, J. Chem. Soc., Faraday Trans. 1 **77**, 2053 (1981).
[23] J. H. Lee, H. B. Lee, and J. D. Andrade, Prog. Polym. Sci. **20**, 1043 (1995).
[24] K. Devanand and J. C. Selser, Macromolecules **24**, 5943 (1991).
[25] E. Florin, R. Kjellander, and J. C. Eriksson, J. Chem. Soc., Faraday Trans. 1 **80**, 2889 (1984).
[26] J. E. Kohn *et al.*, Proc. Natl. Acad. Sci. U.S.A.**101**, 12 491 (2004).
[27] H. P. Hsu, W. Paul, and K. Binder, Europhys. Lett. **92**, 28 003 (2010).